Fluid-induced anthropogenic and natural earthquake swarms driven by aseismic slip

Philippe DANRE[1,1,1], Louis De Barros[2,2,2], Frédéric Cappa[3,3,3], and Jean-Paul Ampuero[4,4,4]

[1]Géoazur
[2]Université Côte d'Azur, CNRS, Obervatoire de la Côte d'Azur, IRD, Géoazur
[3]Université Côte d'Azur, CNRS, Observatoire de la Côte d'Azur, IRD, Géoazur
[4]Institut de Recherche pour le Développement

December 1, 2022

Abstract

Anthropogenic fluid injections at depth induce seismicity which is generally organized as swarms, clustered in time and space, with moderate magnitudes. While some similarities between swarms have already been observed, whether they are driven by the same mechanism is still an open question. Pore fluid pressure or aseismic processes are often proposed to explain observations, while recent models suggest that seismicity is triggered by fluid-induced aseismic slip. Using 22 natural and anthropogenic swarms, we observe that duration, migration velocity and total moment scale similarly for all swarms. This confirms a common driving process for natural and induced swarms and highlights the ubiquity of aseismic slip. We propose a method to estimate the seismic-to-total moment ratio, which is then compared to a theoretical estimation that depends on the migration velocity, the effective stress drop and the slip velocity. Our findings lead to a generic explanation of swarms driving process.

Geophysical Research Letters

Supporting Information for

Fluid-induced anthropogenic and natural earthquake

swarms driven by aseismic slip

Philippe Danré*, Louis de Barros, Frederic Cappa, Jean-Paul Ampuero

*To whom correspondence should be addressed; E-mail: *danre@geoazur.unice.fr*

This document includes:

Supplementary Text S1 to S5 Figs. S1 to S3 Tables S1

Other Supplementary Materials for this manuscript include the following:

Introduction

This Supplementary Material presents information about the data used in our study, the methods chosen to estimate the parameters of interest as well as their limits, and additional figures to help the understanding of the paper.

Text S1. Data

In our study, we used datasets of earthquake swarms from natural and injection-induced origins. Among all the swarms available, we did not consider swarms associated with volcanic activity as they might involve more complex processes (magma circulation, high temperature effects, etc.). We also focus on swarms with suspected fluid-driven processes, excluding swarms that are thought to be purely driven by slow-slips. Furthermore, we did not consider "complex" swarms, i.e. swarms with several phases of activity (bursts of seismicity separated by periods of quiescence for instance) or with several faults involved, as it would make our assumptions for parameter estimations less reliable. We limited our work to simple swarms, with well-located events on a planar structure. Studying complex swarms with our methods could be done by decomposing them into more simple subsets.

The data required for our study only consists in standard earthquake catalogs, which contain origin time, localization and magnitude. For the Soultz 2004 and Cahuilla swarms, we do not have a moment magnitude but only a local magnitude. We assumed, following *(* Edwards and Douglas, 2014*)* that for the first case Mw=Ml-0.2 while we use the relation in Hawthorne et al. (2017) for the Cahuilla swarm.

For some of the swarms studied, the largest event static stress drop value was available in the literature. In this case, we used this value in our work. Otherwise, we assumed a default value of 10MPa.

Some of the sequences have incomplete data. Indeed, for the Soultz 1993 and 1995 swarms, instrumental deficiencies lead to gaps in seismicity. However, given the small temporal duration of those gaps (<10% of the total duration), we chose not to correct for them, and consider the missing seismic moment as negligible at first approximation.

Text S2. Description of the data used.

We briefly describe below the datasets used, the context of injection or of seismic activity as well.

Basel, Switzerland : In 2006 a fluid injection took place in the underground of the city of Basel, in Switzerland. It aimed at developing an Enhanced Geothermal System (EGS). More than 11,000 cubic meters of fluids were injected at a depth of around 5km, during 6 days. After an intense seismic activity, the injection was stopped. Despite that, a Ml=3.4 event took place a few hours after well shut-in, and seismicity was still intense a few days after that. Mainshock stress drop has been to 2MPa (Goertz-Allmann et al., 2011). In our work, we use the relocated catalog from Herrmann et al., 2019.

Soultz-Sous-Foret, France : The 1993, 1995, 1996, 2000, 2003, 2004 Soultz-Sous-Foret fluid injections took place in Alsace, France. Those injections also aim at developing a deep geothermal system. Using several well with time, GPK1-4, injections of 9400 (in 2004) to 37000 (in 2003) cubic meters took place at about 5km, during 4 to 15 days. The largest earthquake induced range from Mw=0.8 for the 1993 sequence to Mw=2.9 for the 2003 sequence. Data for those sequences are provided by the CDGP services (*https://cdgp.u-strasbg.fr/geonetwork/srv/fre/catalog.search#/home*).

Rittershoffen : In June 2013, an hydraulic stimulation took place in Eastern France at a depth of 2580m. It lasted 2 days, and lead to a few hundreds of events, separated into two phases both temporally and spatially (Lengline et al., 2017). We consider both phases as injection-induced sequences, but analyze them independently. We get migration velocities of 251m/day and 1161 m/day, over durations of 0.48 and 0.05 days respectively.

ST1, Finland : This fluid injection is the most recent of our dataset. It took place in June and July 2018 during 49 days. The goal was to control the injection parameters in order to mitigate the associated risk.

A volume of fluids of more than 18,000 cubic meters was injected at a depth of around 6.1 km. It led to several events of magnitude greater than 1 and one of magnitude 1.9. The value of the largest event static stress drop (taken as 20MPa) and the earthquake data comes from *(* Kwiatek et al., 2019*)* .

Paralana, Australia : This injection took place at about 4km below the surface, in the South of Australia, in July 2011. More than 3,000 cubic meters of fluids were injected to create a geothermal reservoir. The induced seismicity presented a mainshock with a magnitude of Mw=2.5. The data are provided by J. Albaric (Albaric et al., 2014) and the static stress drop value for the biggest earthquake is 1.8MPa (*Pers. Communication . from J. Albaric*).

Cooper Basin, Australia : In 2003, an injection was performed in the Cooper Basin injection site in Australia. During ˜45 days, 20000 cubic meters of fluids were injected at a depth of ˜4250m in the granitic crust, during two phases. We only consider here the seismicity between 29/11/2003 and 22/12/2003.

In 2012, around 34000 cubic meters of fluids were injected during two injections (a small one then the main one) in a new well, at ˜4000m depth. We focus here only on the main injection, going on from 17/11/2012, with around 20000 events.

The data for Cooper Basin come from the EPOS repository (*https://tcs.ah-epos.eu/#episodes*:).

Paradox Valley, USA : This sequence is one of the longest injection-induced seismic sequence, as injection activities in this area of the Colorado began in 1985. About 7.7 million cubic meters have been injected at a depth between 4 and 5 km. This tremendous injection lead to several Mw>4 earthquakes like in May 2000 and January 2013. Yeck et al., 2015 estimate the largest event static stress drop as being 5MPa.

Corinth, Greece : The Gulf of Corinth is an extension zone prone to earthquake swarms. The swarm considered here occurred in 2015 and lasted 10 days, with a magnitude culminating at 2.5. The data used come from De Barros et al., 2020.

Ubaye, France : This earthquake swarm began in 2003 in the Alps region in France. It lasted 2 years. The data used is an earthquake catalog of relocated events from Daniel et al., 2011 of more than 1,000 events (more than 16,000 were initially detected by (enatton et al., 2007).

Crevoux, France : This small swarm also occurred in the Alps region, in 2014, just near the Ubaye Valley. It took place during the aftershock sequence of the 07/04/2014 Barcelonette earthquake (Ml=4.8), 6km North of the main cluster of seismicity (De Barros et al., 2019)

SWX, Iceland : The Husavik–Flatey Fault has experienced numerous earthquake swarms (Passarelli et al., 2018). From Passarelli's study, we considered 3 swarms, in 2001, 2008 and 2013, taking place in different zones of the same transform fault. We chose those swarms among the other swarms they studied because of their spatial and temporal simplicity (Passarelli et al., 2018). **Cahuilla, USA :** Similarly to the Ubaye swarm, this swarm is unexpectedly long, lasting more than 2 years and with a highest magnitude of Mw=4.4. It took place near the San Jacinto fault, an area prone to earthquake swarms. Composed of more than 19000 events, the catalog from Ross et al., 2020 was used here.

Text S3. Migration velocity of the swarms

In our study, we estimate the migration velocity of the swarms using the same methodology for both natural and injection-induced sequences. Indeed, if for the latest the injection location can be known and used as the origin for distance computation, it is not available for natural swarms. We therefore decided to take as a spatial origin the median of the coordinates of the first 10 events. Indeed, those 10 first events can be considered close spatially and temporally to the injection point given that hundreds or thousands of events will then migrate from there.

With this spatial origin, and taking the occurrence time of the first event as the t=0s reference, we compute the distance and time of each event. We define the migration front of the swarms based on the 90^{th} percentile of distance bins with time. Indeed, some events, likely background seismicity or mislocated events, occurred isolated at large distances early in the swarm. Choosing the 90^{th} percentile of distance allows us not to take into account those events for the migration velocity computation. For the ST1 swarm velocity fitting, we removed the events happening at a >750m distance very early in the swarm, as they do not seem triggered by the same mechanisms as the other events. The percentiles were computed over sliding 50 events bins, to get a reliable estimate of the position of the seismicity front with time.

For each swarm, we empirically defined a migration period. Indeed, in the case of injection-induced swarms, the seismicity front migration decelerates when the injection is stopped. It is likely to be the case for natural earthquake swarms, but the injection duration is unknown in this case. As we did not find a criterion for natural and injection-induced swarms to separate the migrating and non-migrating part and avoid a bias in the fitting, we empirically defined the migration period as the time during which the migration front propagates. In all cases, this period lasts most of the swarm.

Over the migration period, we then just performed a linear regression over the 90^{th} percentiles of distance with time. The value of the slope is the migration velocity of the swarm. We do not force the fit of the seismic front to pass by the origin as 1) the injection might not be purely punctual, but may originate from a 1D/2D structure, such as an open borehole and 2) the origin time is arbitrarily fixed to occurrence time of the first event time, but the injection might have started before.

This method allows us to get an average migration velocity for all swarms.

We added, on Figure 2, some data from literature. Those sequences come from Kim et al., 2013; Seeber et al., 2004; Duverger et al., 2015 ; Yoshida et al., 2018 ; Duboeuf, 2018.

Text S4. Effective stress drop

Following Fischer et Hainzl, 2017, we compute the effective stress drop of the studied seismic sequences. Some catalogues (Rittershoffen) do not have moment available. In this case, we did not consider them in the computation of the effective stress drop or further for the total moment estimation.

The effective stress drop is defined following the same formalism as the static earthquake stress drop, but at the scale of the swarm and not of the individual earthquake. Therefore, it depicts the cumulative seismic moment release over the seismicity area to the power 3/2 (see Equation S1). Effective stress drops are usually lower than classical values of static earthquake stress drop (1-10 MPa). A low effective stress drop value indicates a low seismic moment release on a large seismicity area, and therefore a strong aseismic deformation. On the contrary, an effective stress drop value that gets close to an earthquake one indicates that most of the slip is seismic. We here do not focus on the possible time variations of the effective stress drop during the swarm but on its final value.

To compute the effective stress drop, we use a similar method as in Fischer et Hainzl, 2017. First, given a set of hypocenters in 3D, we remove the few points too far away from the rest of the seismicity. Then, using a least square fitting method, we find the best plane fitting the 3D distribution of the events. Assuming that all events occured on a single fault, we then project the hypocenters on this plane, and after removing once again the points too far away, we compute the area of seismicity using a Convex Hull.

Note that it is important to remove the outliers as (i) they could bias the plane fitting and (ii) they can lead to an overestimation of the seismicity area and radius (especially given that to compute the effective stress drop we need a cubic power of the radius).

We then sum the seismic moment of the events within the area, and compute a radius by assuming the area of seismicity is circular, following :

$$R = \sqrt{S/\pi}$$

The effective stress drop [?]σe is given by (24) following :

$\Delta\sigma_e = \frac{16 * M_{0,seismic}}{7 * R^3}$ (Equation S1)

where $M_{0,seismic}$ is the cumulative seismic moment. We find similar values to the ones previously determined by *(24),* like 0.95 MPa and 3 MPa for Basel, or 0.36 MPa and 0.34 MPa for Soultz 2000 (our analysis and Fischer et Hainzl, 2017 respectively*)* Those differences can come from the difference in the catalogs used (i.e. differences in cumulative moment values, localization of the events, etc.) or from the implemented methods.

Text S5. Total moment

To compute the total moment, we consider the slip$\mathbf{D}_{\max}$ over the main event asperity. We compute$\mathbf{D}_{\max}$ based on the main event moment and stress drop. We neglect the afterslip given that aseismic slip represents only ˜20% of the slip occurring over the seismically slipping area for simulations of small repeating earthquakes (Chen et Lapusta, 2009). Therefore, we can still get the good order of magnitude for the slip occurring over the seismically slipping area by not considering aseismic slip.

On Figure 4 in the main text, the indicative black lines were computed assuming a G value of 30GPa and $V_{\max}/n$ values of10^{-9}, 10^{-8} and 10^{-7}m/s values. To see the influence of the value of G on the estimated values of $V_{\max}$ we plot below the same figure but with G=15GPa. Despite a lateral shift, we still find similar values, consistent, for $V_{\max}/n$.

Fig. S1.

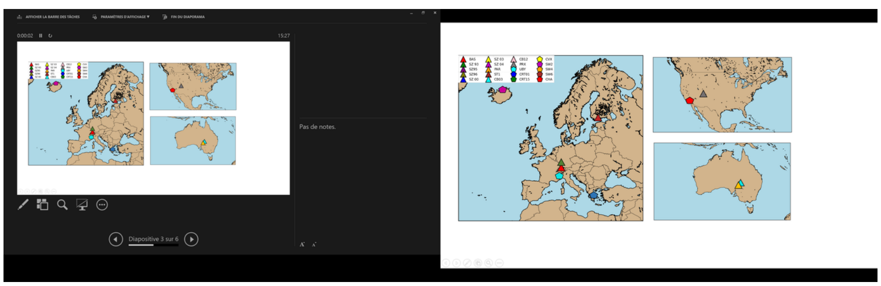

Figure S1 : Map with the locations of the swarms studied. Symbols and color are the same as in the main manuscript. When swarm location is redundant, only one symbol is represented.

Fig. S2.

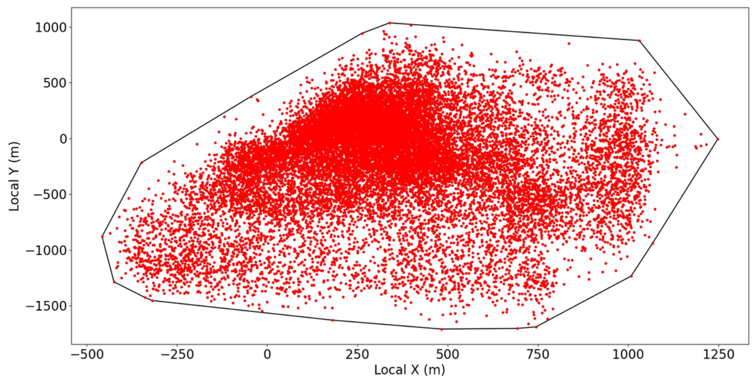

Figure S2 : Area computation in the case of the Cooper Basin sequence. After removing the too far away points (none here), area is computed using a Convex Hull algorithm, which computes the smallest convex envelope that encloses all the seismic events, projected on the best-fitting fault plane.

Fig. S3.

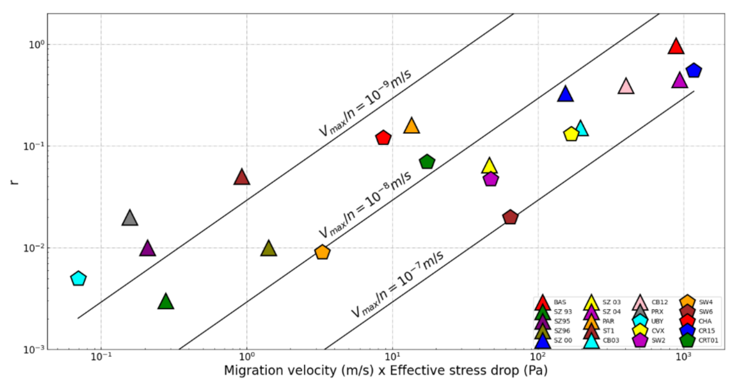

Figure S3: Seismic to total moment ratio as a function of the product of the swarm migration velocity and its effective stress drop. Here a value of G=15GPa is assumed.

Table S1.

Name	Data source	Migration duration (
Basel (BAS)	Herrmann et al., 2019	6.7
Soultz 1993 (SZ93)	*EOST & GEIE EMC. (2017), CSMA;* Bourouis and Bernard, 2007	15.5

Name	**Data source**	**Migration duration (**
Soultz 1995 (SZ95)	*EOST & GEIE EMC. (2017), CSMA;* Gerard et al., 1997	11.6
Soultz 1996 (SZ96)	*EOST & GEIE EMC. (2017), CSMA;* Gerard et al., 1997	2.1
Soultz 2000 (SZ00)	*EOST & GEIE EMC. (2018),* Cuenot et al., 2008	7.3
Soultz 2003 (SZ03)	*EOST & GEIE EMC. (2018),* Calo and Dorbath, 2013	17.9
Soultz 2004 (SZ04)	*EOST & GEIE EMC(2018);* Dyer et al., 2004	2.4
Paralana (PAR)	Albaric et al., 2014	6.0
ST1	Kwiatek et al., 2019	47.3
Cooper Basin 2003 (CB03)	Baisch et al., 2006	11.6
Cooper Basin 2012(CB12)	Baisch et al., 2015	15.8
Paradox (PRX)	*US Bureau of Reclamation*	8815
Ubaye (UBY)	Daniel et al., 2011	658
Corinth 2001	Duverger et al., 2018	150
Corinth 2015 (CRT)	De Barros et al., 2020	5.0
Crevoux (CRV)	De Barros et al., 2019	6.3
SW2	Passarelli et al., 2018	20
SW4	Passarelli et al., 2018	12.8
SW6	Passarelli et al., 2018	11.4
Cahuilla (CHA)	Ross et al., 2020	1073

Table S1 : Results of our computations. * = Cumulative seismic moment within the area determined for the effective stress drop. It might differ from the cumulative seismic moment of the whole catalog.

Fluid-induced anthropogenic and natural earthquake swarms driven by aseismic slip

Philippe Danré [1*], Louis De Barros [1], Frédéric Cappa [1,2], Jean-Paul Ampuero[1]

[1] Université Côte d'Azur, CNRS, Observatoire de la Côte d'Azur, IRD, Géoazur, France

[2] Institut Universitaire de France, Paris

Corresponding author: Philippe Danré (danre@geoazur.unice.fr)

Key Points:

- Scaling laws show that injection-induced and natural earthquake swarms have the same driving mechanism.
- We show that aseismic slip is always present in swarms, although its contribution differs from one swarm to another.
- We propose a model based on fluid-induced aseismic slip propagation that explains swarms behavior.

Abstract

Anthropogenic fluid injections at depth induce seismicity which is generally organized as swarms, clustered in time and space, with moderate magnitudes. While some similarities between swarms have already been observed, whether they are driven by the same mechanism is still an open question. Pore fluid pressure or aseismic processes are often proposed to explain observations, while recent models suggest that seismicity is triggered by fluid-induced aseismic slip. Using 22 natural and anthropogenic swarms, we observe that duration, migration velocity and total moment scale similarly for all swarms. This confirms a common driving process for natural and induced swarms and highlights the ubiquity of aseismic slip. We propose a method to estimate the seismic-to-total moment ratio, which is then compared to a theoretical estimation that depends on the migration velocity, the effective stress drop and the slip velocity. Our findings lead to a generic explanation of swarms driving process.

Plain Language Summary

Swarms are a particular type of seismic sequence, during which many earthquakes occur but with no mainshock distinguishable from the other events. They can be induced by anthropic injections at depth, like during geothermal exploitation. Natural swarms are also observed in a large variety of geological contexts. Natural and injection-induced swarms share a lot of similarities, like the migration of seismicity. But little is still known about their physics. Here, we explain the observed similarities by the fact that both types of swarms correspond to earthquakes triggered by the propagation of an aseismic slip transient, induced by fluid circulation. This allows to reconcile observations made over different length- and timescales, and provides a generic explanation of the processes occurring at depth.

1. Introduction

1.1 Natural and injection-induced swarms exhibit many similarities

Fluid pressure changes at depth can induce seismicity, as shown by the increase in seismicity near fluid injection sites during geothermal activities (e.g., in Basel, Switzerland; Diechmann and Giardini, 2009), wastewater storage in Oklahoma (Hincks et al., 2018), or during fault activation experiments in France (Guglielmi et al., 2015). On the other hand, earthquake swarms of natural origin (i.e., sequences of clustered earthquakes with moderate magnitudes, generally below $M_w = 5$, without a mainshock-aftershock pattern) occur in various geological and tectonic contexts, such as mountain ranges (Jenatton et al., 2007), rift zones (De Barros et al., 2020) or along transform faults (Roland and McGuire, 2009). Earthquakes during those swarms are located over one or several fault planes *(*Lohman et McGuire, 2007; Baisch et al., 2009: Hong et al., 2020; Fischer et Hainzl, 2021*).* Migration of seismicity is the most characteristic behavior of both injection-induced and natural earthquake swarms (Goebel et Brodsky, 2018*;* Passarelli et al., 2018). Proposed physical explanations for swarm migration include fluid pressure diffusion (Shapiro et al., 1997), aseismic slip (Roland et McGuire, 2009), or a combination of both (De Barros et al., 2021), as well as cascading events (Fischer et Hainzl, 2021).

To gain deeper understanding into swarm processes and evaluate how generic they are, we compare injection-induced swarms with natural ones. Given the similarities identified between the two types of swarms, we aim at evaluating if a common mechanical process may drive swarms in different geological contexts and origins.

1.2 Understanding the role of aseismic slip in swarms

Aseismic moment release is thought to occur for injection-induced sequences, as revealed by moment-volume scaling relations (McGarr et Barbour, 2018*;* De Barros et al., 2019), by geodesy in the vicinity of a fluid injection site in the Brawley Basin (Wei et al., 2015), by measurements during field experiments (Guglielmi et al., 2015) or indirectly by studying repeating earthquakes during the Soultz-Sous-Forêt sequences (Bourouis and Bernard, 2007; Lengliné et al., 2014). The relatively weak values of seismic moment released compared to the spatial extent of seismicity also indicate that aseismic slip occurs over the whole seismicity area (Fischer and Hainzl, 2017). Aseismic slip has also been observed in association with natural swarms, using geodesy and slip inversions (Lohman and McGuire, 2007; Gualandi et al., 2017), or by studying dual velocity migrations and repeating earthquakes during the 2015 swarm in the Gulf of Corinth (De Barros et al., 2020). Nevertheless, geodetic observations of aseismic slip associated with swarms remain rare and difficult to achieve, given the depth, long duration and low deformation of such sequences.

Numerical modeling showed that the increase of the critical earthquake nucleation size with fluid pressure first leads to aseismic slip, which may outpace the diffusing pressure front (Bhattacharya and Viesca, 2019; Larochelle et al., 2021) and which triggers seismicity near its edges where shear stresses increase (Cappa et al., 2019; Wynants-Morel et al., 2020*)*.

As illustrated on Figure 1, and based on the previously mentioned observations, while aseismic slip is directly induced by fluid pressure, earthquake swarms seem to be triggered by the shear stress perturbation resulting from aseismic slip propagation over brittle asperities, rather than by fluid overpressure. In this case, seismicity migration would be related to the aseismic slip propagation, and not to the diffusion of fluids (Bhattacharya et al., 2019; De Barros et al., 2021).

This is analogous to the observed co-location of seismic and aseismic slip areas during large slow slip events (SSEs) in subduction zones, as in Cascadia (Bartlow et al., 2011). The seismic events (tremors or earthquakes) are triggered by the stress transfer from the SSEs, even though such SSEs are not necessarily driven by pore fluid pressure perturbation.

In this work, we aim at exploring the similairities between injection-induced sequences and natural swarms in a general way, in order to infer if both types of seismicity can be explained by a common process, and in which extent aseismic slip is driving them. Using a dataset of 22 seismic sequences, we first investigate scaling relations between moment, migration and duration and we compare them to slow-slip events observations. As aseismic slip seems to be a common feature among swarms, we then introduce a method to estimate the total and aseismic deformation. Finally, we propose a mechanical framework that relates the seismic to total ratio to seismic observables.

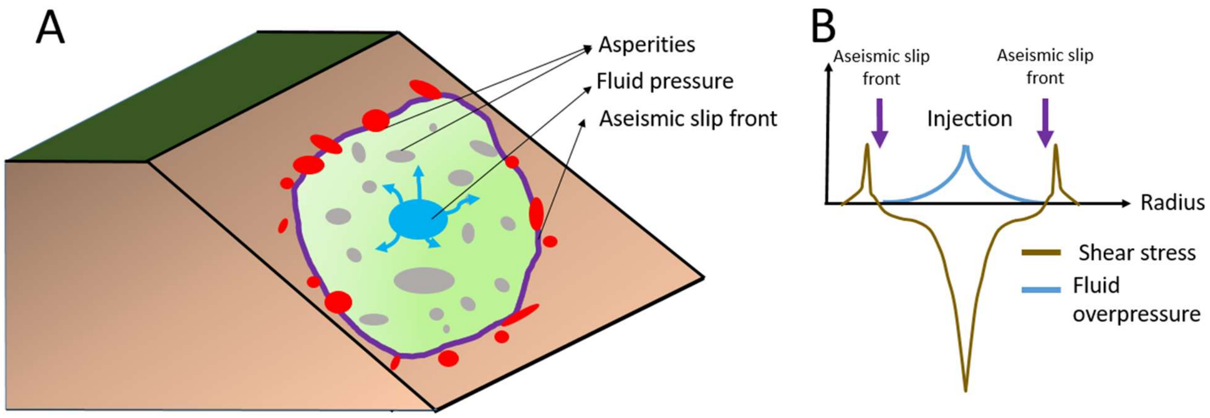

Figure 1. Common model for natural and induced swarms. (A) Conceptual view. Over a fault plane, fluid overpressure (blue arrows), either from anthropogenic or natural origin, induces aseismic slip (light green area). As the aseismic slip zone expands, it triggers seismicity near its edges (red patches) or within it (grey patches), through shear stress perturbation (brown curve, right). (B) Shear stress and fluid overpressure versus radial distance to the injection. The fluid overpressure induces an aseismic slip, with a shear stress drop within the slipping area and a stress concentration at its tip.

2. Materials and Methods

2.1 Data

We focus on a global dataset of 22 earthquake swarms, from either injection-induced or natural origin. For natural sequences, geological contexts are diverse: for instance, the 2003-2004 Ubaye swarm (Jenatton et al., 2007) occurs in a near-zero strain-rate area in the French Alps, while the 2015 Corinth swarm (De Barros et al., 2020) takes place in a very fast extensional (~15 mm/year) rift zone in Greece. We here focus on natural swarms in which fluid processes have been previously discussed, and we do not consider swarms taking place near volcanoes or in subduction zones. Most of the injection-induced swarms we consider originated from geothermal exploitation. However, they span a wide range of characteristics, including the injected fluid volume and the injection depth (see Supp.).

2.2 Migration velocity

Migration velocity of the 22 swarms is computed by fitting the seismicity front. Migration period is defined as the time during which the swarm is expanding. The spatial origin is chosen as the median of the coordinates of the 10 first events, and the origin time is defined as the time of the first event. We define the seismicity front as the 90th percentile of event distances in a sliding window containing 50 events. Seismicity front has been modelled by either diffusive law, linear fit or more complex relationships (Goebel et Brodsky, 2018; De Barros et al., 2021). The shape of the migration is here not investigated, as we only focus on an average migration velocity, in order to make comparisons among the different swarms. We fit a linear model over the seismicity front during the migration period of each sequence. This procedure yields migration durations and average migration velocities for each sequence (Figure 2A,B).

2.3 Seismicity area and effective stress drop computation

By analogy with the moment-size relationship for circular ruptures, the effective stress drop of a swarm is defined as (Fischer et Hainzl, 2017):

$$\boldsymbol{\Delta\sigma_e} = \frac{\boldsymbol{7M_{0,seismic}}}{\boldsymbol{16R^3}} \quad \text{(Equation 1)}$$

where R is the radius of the seismicity area and $\boldsymbol{M_{0,seismic}}$ the seismic moment released during the swarm. The effective stress drop value is an indicator of the relative importance of aseismic moment release (Fischer and Hainzl, 2017): a low effective stress drop suggests distant seismic asperities embedded in a fault slipping aseismically, while values close to earthquake static stress drops suggest that seismic asperities cover most of the slipping area.

Following Fischer and Hainzl (2017), seismicity area is computed by fitting a 2D plane over the 3D distribution of hypocenters, after removing the outsiders biasing the plane fitting. Hypocenters are then projected over the plane, and a ConvexHull algorithm delineates and returns the seismicity area S. We then compute a characteristic size, defined as $\boldsymbol{R} = \sqrt{\boldsymbol{S/\pi}}$, and with the cumulative seismic moment value, we compute the effective stress drop.

2.4 Total moment estimation

Aseismic slip quantification is difficult for injection-induced sequences as deformations associated with those episodes are small (0.5mm for the Guglielmi et al., 2015 field experiment), over long durations, leading to small strain rates hard to observe. This issue stays the same for natural swarms.

We here propose a simple way to estimate, roughly, the aseismic slip. Studies of slow slip transients have shown that the slip released by repeating earthquake sequences equals the surrounding aseismic slip (Matsuzawa et al., 2004; Uchida, 2019). As the front of the swarm seismicity is assumed to be directly triggered by the shear stress perturbation induced by aseismic slip (Figure 1), we here make an analogy with slow slip transients. We suppose that the slip released seismically over discrete asperities equals the surrounding aseismic slip and neglect the afterslip (see Supp.). Assuming the asperity associated with the largest earthquake in the swarm only ruptures once, its slip gives an order of magnitude of the slip over the whole area. For each sequence, we isolate the largest event of moment $\boldsymbol{M_{0,max}}$ and assuming a circular rupture with a static stress drop $\boldsymbol{\Delta\sigma_{max}}$ of 10MPa (unless a more precise value is provided in the literature, see Supp.), we compute the slip $\boldsymbol{D_{max}}$ over this asperity (Madariaga, 1976) as:

$$\boldsymbol{D_{max} = M_{0,max}^{1/3} * \frac{(16\Delta\sigma_{max})^{2/3}}{G\pi 7^{2/3}}} \text{ (Equation 2)}$$

Given that seismic moment is released over brittle asperities and aseismic slip is released in between them, we estimate the total moment (seismic + aseismic) over the seismicity area as

$$\boldsymbol{M_{0,total} = G * D_{max} * S} \text{ (Equation 3)}$$

where G is the rock shear modulus (taken here as 30 GPa) and S the previously computed seismicity area. While the effective stress drop qualitatively indicates the importance of aseismic slip during a swarm, the rough quantification approach here allows us to better constrain aseismic moment release for each sequence.

2.5 Seismic to total moment ratio

By considering seismic and aseismic slip into one single slip event over a circular area of radius R, we have (Madariaga, 1976):

$$\boldsymbol{M_{0,total} = \frac{16}{7}\Delta\sigma_{total}R^3} \text{ (Equation 4)}$$

Where $\boldsymbol{\Delta\sigma_{total}}$ is the total stress drop over the studied area.

The rupture velocity of slow slip events is related to its stress drop and to its maximum slip velocity $\boldsymbol{V_{max}}$ (Ampuero and Rubin, 2008; Rubin, 2008; Passelègue et al., 2020) with:

$$\boldsymbol{V_{rupt}} = \frac{\boldsymbol{G*V_{max}}}{\boldsymbol{n*\Delta\sigma_{total}}} \text{ (Equation 5)}$$

To establish this, we assume that the stress drop of the slip event, $\boldsymbol{\Delta\sigma_{total}}$, is proportional (factor n > 1) to the associated strength drop. This can be observed in several numerical simulations of slow slip, where n~10 (Hawthorne and Rubin, 2013; Lambert et al., 2021).

In our case, we make the hypothesis that the seismicity is triggered by the fluid-induced aseismic slip. Therefore, the seismicity front follows the aseismic front (Wynants-Morel et al., 2020). The migration velocity of the swarms is then the rupture velocity of the aseismic slip ($V_{rupt} = V_{migr}$). Combining Equation 4 and Equation 5 we then have:

$$\boldsymbol{M_{0,total}} = \frac{\boldsymbol{16}}{\boldsymbol{7}} * \frac{\boldsymbol{G*V_{max}}}{\boldsymbol{n*V_{migr}}} * \boldsymbol{R^3} \text{ (Equation 6)}$$

This leads us to the following expression for the ratio *r* of seismic to total moment:

$$\boldsymbol{r} = \frac{\boldsymbol{M_{0,seismic}}}{\boldsymbol{M_{0,total}}} = \frac{\boldsymbol{7*M_{0,seismic}}}{\boldsymbol{16*R^3}} \frac{\boldsymbol{n*V_{migr}}}{\boldsymbol{G*V_{max}}} \text{ (Equation 7)}$$

This equation can be written in a more compact form using the effective stress drop (see Equation 1). We then get:

$$\boldsymbol{r} = \frac{\boldsymbol{n*\Delta\sigma_e*V_{migr}}}{\boldsymbol{G*V_{max}}} \text{ (Equation 8)}$$

This relation links the ratio of the cumulative seismic to total moment to the product of the migration velocity and the effective stress drop of the swarm.

3. Results

3.1 Aseismic slip drives the swarm's dynamics

The estimated velocities for the 22 swarms studied here range between a few meters per day, like for the Cahuilla swarm (Ross et al., 2020), to more than 1 km/day in the case of the Rittershoffen sequence (Lengliné et al., 2017). Figure 2C shows the migration velocity as a function of duration, for induced and natural swarms. For sake of comparison, we add the migration velocity of SSEs recorded on subduction zones (Gao et al., 2012). For these events, velocities correspond to the propagation of an aseismic slip, which is characterized either with geodesy (Schmidt and Gao, 2010) or with tremor migration (Bartlow et al., 2011; Ito et al., 2007).

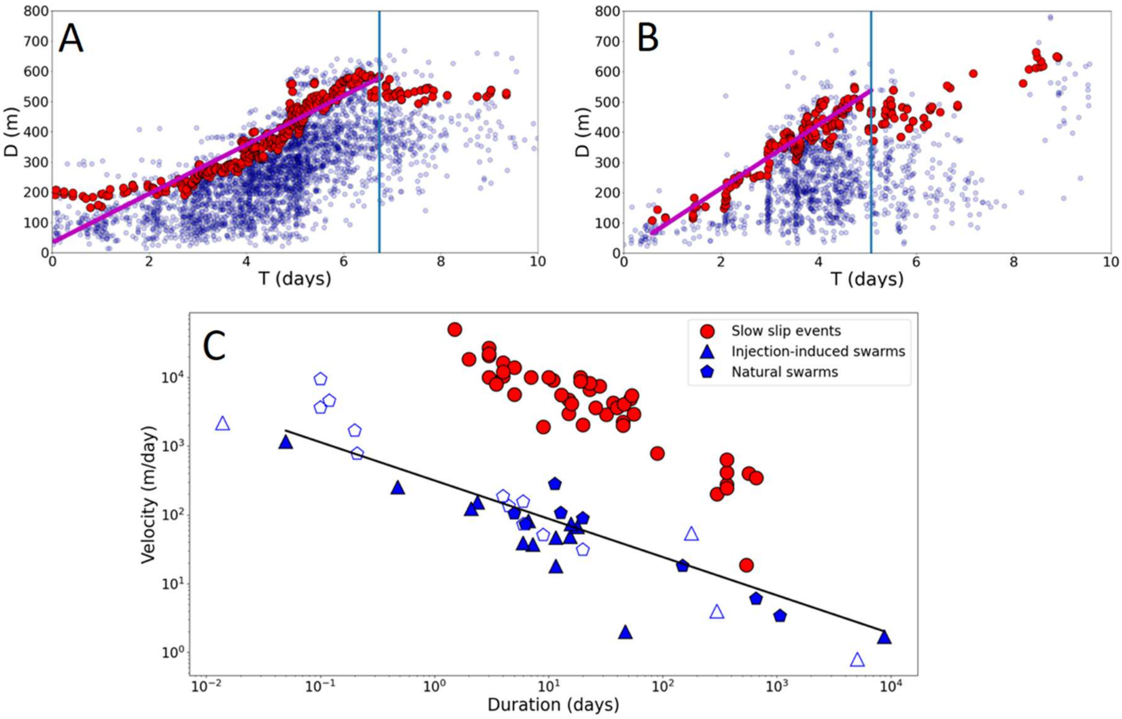

Figure 2. Scaling of propagation velocity with duration for swarms and slow slip events (SSEs). (**A**) Space-time distribution of seismicity in the Basel sequence (Herrmann et al., 2019*)*. Blue dots represent individual event hypocenters while red circles represent the computed seismicity front. Linear fitting (magenta line) over the seismicity migration period, delimited by the vertical blue line, yields a propagation velocity of 81 m/day. (**B)** Same but for the Corinth 2015 swarm (De Barros et al., 2020). The seismicity front migrates at a velocity of 105 m/day. (**C)** Scaling of

velocity with duration. Red dots represent SSE data from (Gao et al., 2012). Filled triangles and pentagons represent injection-induced and natural swarms, respectively, for which we determined migration velocity and duration based on seismicity catalogs. Empty symbols represent migration velocities and durations directly taken from the literature (see Supp.). Black line represents the best-fitting line between our computed velocities and durations ($R^2 = 0.76$).

Two main observations can be made. First, injection-induced and natural swarms follow the same scaling $\boldsymbol{V \alpha\, T^{-\gamma}}$ of velocity with duration, with $\boldsymbol{\gamma = 0.6}$ and $\boldsymbol{\gamma = 0.7}$ when considering each subset individually. In addition to the other similarities discussed beforehand, the continuous scaling of velocity with duration for all swarms is direct evidence that both types of sequences obey the same physics for all velocity ranges (from a few meters per day in Ubaye or Cahuilla to 1160 m/day for Rittershoffen). As anthropogenic seismicity is induced (though indirectly) by fluid injection (Bentz et al., 2020), this confirms that natural swarms are also a consequence of fluid pressure perturbations.

Second, the velocity-duration scaling is the same for swarms and for the SSEs reported by Gao et al. (2012), despite higher velocities for the latter, typically around 1 to 10 km/day. This confirms that the migration of swarms globally behaves as the propagation of aseismic slip, hence the assumption made of $V_{rupt} = V_{migr}$. The observed scaling for swarms, $\boldsymbol{V \alpha T^{-\gamma}}$ with $\boldsymbol{\gamma = 0.55}$, is compatible with fluid diffusion. However, a similar scaling is obtained for SSEs, which exhibit individual linear migrations (Houston et al., 2011) and are not driven by fluid diffusion. Other mechanisms have been proposed to explain such a scaling for SSEs, like a uniform stress drop or a uniform slip (Ide et al., 2007). These mechanisms might also be valid for swarms, explaining then the observed continuum of characteristics (Figure 2C). Therefore, a general scaling compatible with diffusion does not imply that individual swarm are directly driven by fluid diffusion.

The effective stress drop $\boldsymbol{\Delta\sigma_e}$ is found to range between 1 kPa and 1 MPa (Figure 3). Those values are lower than typical values of static stress drop for earthquakes, which usually range between 1 and 100 MPa (Cocco et al., 2016) and are more similar to the stress drop values of SSEs (Brodsky and Mori, 2007). Thus, they indicate an aseismic component in the swarm processes. For instance, $\boldsymbol{\Delta\sigma_e}$ =1kPa for the Soultz-sous-Forêt stimulation, indicates an important aseismic moment release, while $\boldsymbol{\Delta\sigma_e}$ = 1MPa for the Basel injection means that aseismic slip is relatively less important in this case. $\boldsymbol{\Delta\sigma_e}$ ranges in a similar way for natural and injection-induced sequences (Figure 3), indicating once again that mechanisms of seismic and aseismic moment release are controlled by the same processes for both types of sequences.

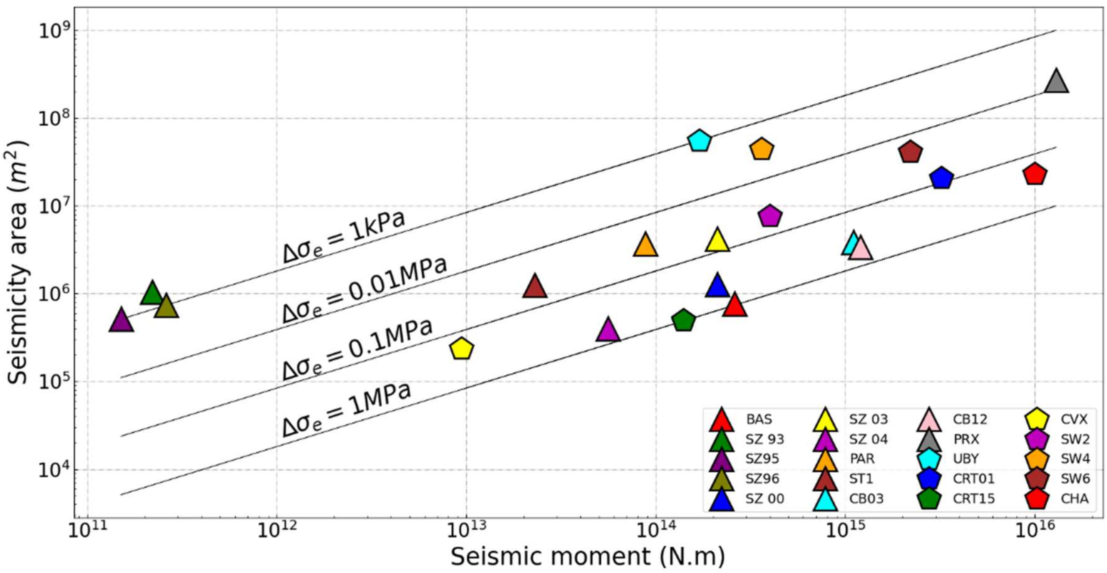

Figure 3. Seismicity area (m²) as a function of the cumulative seismic moment released during 20 of the swarms studied here. Triangles correspond to injection-induced sequences while pentagons refer to natural swarms. Black lines represent different values of the effective stress drop $\boldsymbol{\Delta\sigma_e}$.

Based on migration velocity and effective stress drop analysis, both natural and injection-induced swarms seem to share the same driving processes, in which aseismic slip seems ubiquitous, like depicted on Figure 1. The seismicity front is depicting the aseismic slip rupture propagation and the seismicity area corresponds to the aseismic slip area, in a similar way as tremors locations in SSEs zones delineate slip migration and area (Bartlow et al., 2011). However, the aseismic contribution might be different from one swarm to another.

3.2 Aseismic contribution differs among swarms

Once the total moment $\boldsymbol{M_{0,total}}$ for each swarm is computed, we compare it to the seismic moment released by using the seismic to total moment ratio *r* (Equation 7).

A value of r close to 1 indicates that moment release is mainly seismic, while a lower value shows that moment release is significantly aseismic. We compute $\boldsymbol{M_{0,total}}$ and *r* for the swarms studied here. As shown in Figure 4A, *r* ranges from 0.001 to almost 1. For the Basel injection-induced sequence, *r* = 0.97, suggesting that aseismic deformation is low in this case, while for the Ubaye natural swarm, r = 0.005, indicating an important aseismic moment release.

For the Soultz 1993 sequence, despite an injected fluid volume of the same order of magnitude as in the Basel injection (Diechmann et Giardini, 2009), the cumulative seismic moment is 3 orders of magnitude lower than the Basel one. This can be explained here by an important aseismic moment release (r ~ 0.001) taking place during the Soultz sequence. Therefore, the strong difference of seismic moment release for similar volumes can simply reflect the amount of induced aseismic deformation (McGarr and Barbour, 2018; De Barros et al., 2019).

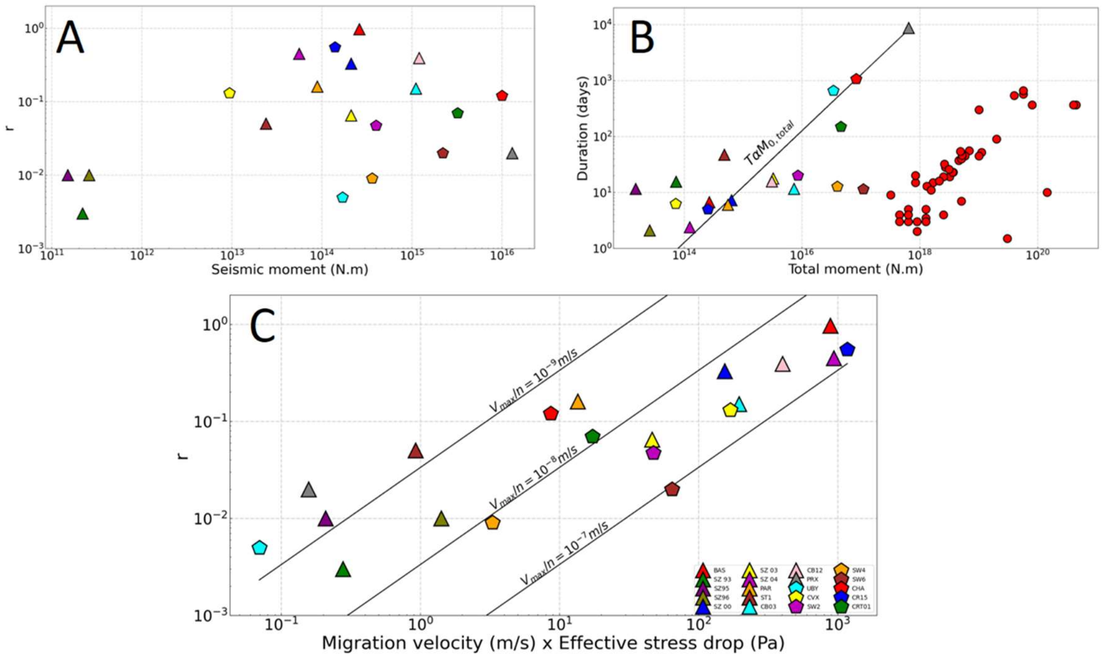

Figure 4. (**A**) Seismic to total moment ratio, as a function of the seismic moment released during each swarm, for the sequences studied here. (**B**) Duration as a function of the estimated total moment. Black line represents the 1:1 scaling. Red dots correspond to the SSE data from Gao et al., 2012. (**C**) Seismic to total moment ratio for the swarms studied here, as a function of the product of the migration velocity and the effective stress drop. The black lines correspond to different values of $\frac{V_{max}}{n}$, assuming G = 30GPa (see Equation 8).

Interestingly, one can also note that the scaling of duration with estimated total moment (Figure 4B) seems to be 1:1, similarly to the scaling between event duration and aseismic moment observed for SSEs (Ide et al., 2007; Peng and Gomberg, 2010), while seismic moment vs duration does not exhibit such a scaling (Passarelli et al., 2018). Indeed, with our total moment estimate, we are able to measure the "hidden" aseismic slip release. As hypothesized (Peng and Gomberg, 2010), the apparent branching off of the swarms in the moment duration can be corrected when considering the aseismic deformation.

Using Equation 8, we can relate the seismic to total moment ratio to two observables, effective stress drop and migration velocity (see Figure 4C). Following Equation 8, we estimate $\boldsymbol{V_{max}/n}$ being between $\mathbf{10^{-10}}$ and $\mathbf{10^{-7}}$ m/s, which is consistent with expected orders of magnitudes (Roland and McGuire, 2009; Glowacka et al., 2001) if we consider a value of n~10 (Hawthorne and Rubin, 2013; Lambert et al., 2021). Variability in $\boldsymbol{V_{max}}$ explains why the observed scaling between $\boldsymbol{r}$ and $\boldsymbol{\Delta\sigma_e * V_{migr}}$ is not as linear as expected. As the general trend shows a scaling different than the isovalues of V_{max}/n, it means that V_{max} also depends, through fault and stress properties, on the seismic-to-total seismic ratio. The slip velocity, together with the migration velocity and the effective stress drop, are the crucial parameters to characterize the seismic and aseismic moment partitioning in swarms. Among other properties, these three parameters depend on the stress state and on the proximity of the fault to failure (Hainzl and Fischer, 2002; Fischer and Hainzl, 2017; Passelègue et al., 2020; Wynants-Morel et al., 2020; De Barros et al., 2021). These relationships therefore deserve to be investigated in order to anticipate the swarm evolution, especially given that similarities are found between swarms and foreshock sequences of some major earthquakes (Chen and Shearer, 2013).

4. Conclusions

In this work, we confirmed that injection-induced and natural swarms are governed by the same physics, as was previously shown for particular sequences (Fischer and Hainzl, 2017). By analyzing sequences covering a wide range of geological contexts, migration velocities, durations and injected fluid volumes, we showed a global unity in the swarm's dynamics. After confirming that fluid-induced aseismic slip explains observations made on swarms, like their migration or their spatial seismic moment release, we exploited the similarities between swarms and slow slip events to introduce a simple mechanical framework that relates the seismic and aseismic moment partitioning to physical and observable parameters (Equation 8). This opens interesting perspectives to better understand swarms, their propagation, and improve their monitoring in order to anticipate potential large earthquakes. It also paves a way to studying natural and injection-induced swarms as the same phenomena.

Acknowledgments

Data for the Iceland swarms were kindly made available by the Icelandic Meteorological Office (SIL) and L. Passarelli (Passarelli et al., 2018). Data from the Paralana sequence and from the Ubaye swarm were made available by J. Albaric (Albaric et al., 2014*)* and G. Daniel (Daniel et al., 2011) respectively. Magnitudes for the Cahuilla swarm were provided by Z. Ross and D. Trugman (Ross et al., 2020). Data for the Soultz fluid injections are available on the CDGP web services. Data for the Cooper Basin injections are available on the EPOS platform. Data for the Paradox Valley fluid injection are available on the US Bureau of Reclamation.

References

Albaric, J., Oye, V., Langet, N., Hasting, M., Lecomte, I., Iranpour, K., ... & Reid, P. (2014). Monitoring of induced seismicity during the first geothermal reservoir stimulation at Paralana, Australia. *Geothermics*, *52*, 120-131.

Ampuero, J. P., & Rubin, A. M. (2008). Earthquake nucleation on rate and state faults–Aging and slip laws. *Journal of Geophysical Research: Solid Earth*, *113*(B1).

Baisch, S., Weidler, R., Vörös, R., Wyborn, D., & de Graaf, L. (2006). Induced seismicity during the stimulation of a geothermal HFR reservoir in the Cooper Basin, Australia. *Bulletin of the Seismological Society of America*, *96*(6), 2242-2256.

Baisch, S., Vörös, R., Weidler, R., & Wyborn, D. (2009). Investigation of fault mechanisms during geothermal reservoir stimulation experiments in the Cooper Basin, Australia. *Bulletin of the Seismological Society of America*, *99*(1), 148-158.

Baisch, Stefan and Rothert, Elmar and Stang, Henrik and Vörös, Robert and Koch, Christopher and McMahon, Andrew (2015) *Continued Geothermal Reservoir Stimulation Experiments in the Cooper Basin (Australia).* Bulletin of the Seismological Society of America, 105 (1). pp. 198-209

Bartlow, Noel M., et al. "Space-time correlation of slip and tremor during the 2009 Cascadia slow slip event." *Geophysical Research Letters* 38.18 (2011).

Bentz, S., Kwiatek, G., Martínez-Garzón, P., Bohnhoff, M., & Dresen, G. (2020). Seismic moment evolution during hydraulic stimulations. *Geophysical Research Letters*, *47*(5), e2019GL086185.

Bhattacharya, P., & Viesca, R. C. (2019). Fluid-induced aseismic fault slip outpaces pore-fluid migration. *Science*, *364*(6439), 464-468.

Bourouis, S., & Bernard, P. (2007). Evidence for coupled seismic and aseismic fault slip during water injection in the geothermal site of Soultz (France), and implications for seismogenic transients. *Geophysical Journal International*, *169*(2), 723-732.

Brodsky, E. E., & Mori, J. (2007). Creep events slip less than ordinary earthquakes. *Geophysical Research Letters*, *34*(16).

Calò, M., & Dorbath, C. (2013). Different behaviours of the seismic velocity field at Soultz-sous-Forêts revealed by 4-D seismic tomography: case study of GPK3 and GPK2 injection tests. *Geophysical Journal International*, *194*(2), 1119-1137.

Cappa, F., Scuderi, M. M., Collettini, C., Guglielmi, Y., & Avouac, J. P. (2019). Stabilization of fault slip by fluid injection in the laboratory and in situ, Sci.

Chen, T., & Lapusta, N. (2009). Scaling of small repeating earthquakes explained by interaction of seismic and aseismic slip in a rate and state fault model. *Journal of Geophysical Research: Solid Earth*, *114*(B1).

Chen, X., Shearer, P. M., & Abercrombie, R. E. (2012). Spatial migration of earthquakes within seismic clusters in Southern California: Evidence for fluid diffusion. *Journal of Geophysical Research: Solid Earth*, *117*(B4).

Chen, X., & Shearer, P. M. (2013). California foreshock sequences suggest aseismic triggering process. *Geophysical Research Letters*, *40*(11), 2602-2607.

Cocco, M., Tinti, E., & Cirella, A. (2016). On the scale dependence of earthquake stress drop. *Journal of Seismology*, *20*(4), 1151-1170.

Cuenot, N., Dorbath, C., & Dorbath, L. (2008). Analysis of the microseismicity induced by fluid injections at the EGS site of Soultz-sous-Forêts (Alsace, France): implications for the characterization of the geothermal reservoir properties. *Pure and Applied Geophysics*, *165*(5), 797-828.

Daniel, G., et al. (2011), Changes in effective stress during the 2003–2004 Ubaye seismic swarm, France, *J. Geophys. Res.*, 116, B01309

De Barros, L. ,Guglielmi, Y., Rivet, D., Cappa, F., Duboeuf, L. (2018). Comptes Rendus Geoscience 350, 464 Invited contributions by 2016–2017 geoscience laureates of the French Academy of Sciences.

De Barros, L., Baques, M., Godano, M., Helmstetter, A., Deschamps, A., Larroque, C., & Courboulex, F. (2019). Fluid-induced swarms and coseismic stress transfer: A dual process highlighted in the aftershock sequence of the 7 April 2014 earthquake (Ml 4.8, Ubaye, France). *Journal of Geophysical Research: Solid Earth*, 124, 3918– 3932.

De Barros, L., Cappa, F., Guglielmi, Y., Duboeuf, L., & Grasso, J. R. (2019). Energy of injection-induced seismicity predicted from in-situ experiments. *Scientific reports*, *9*(1), 1-11.

De Barros, L., Cappa, F., Deschamps, A., & Dublanchet, P. (2020). Imbricated aseismic slip and fluid diffusion drive a seismic swarm in the Corinth Gulf, Greece. *Geophysical Research Letters*, *47*(9), e2020GL087142.

De Barros, L., Wynants-Morel, N., Cappa, F., & Danré, P. (2021). Migration of fluid-induced seismicity reveals the seismogenic state of faults. *Journal of Geophysical Research: Solid Earth*, 126, e2021JB022767.

Deichmann, N., & Giardini, D. (2009). Earthquakes induced by the stimulation of an enhanced geothermal system below Basel (Switzerland). *Seismological Research Letters*, *80*(5), 784-798.

Duboeuf, L. (2018). *Injections de fluide dans une zone de faille (LSBB, Rustrel): sismicité induite et déformation asismique* (Doctoral dissertation, Université Côte d'Azur).

Duverger, C., Godano, M., Bernard, P., Lyon-Caen, H., & Lambotte, S. (2015). The 2003–2004 seismic swarm in the western Corinth rift: Evidence for a multiscale pore pressure diffusion process along a permeable fault system. *Geophysical Research Letters*, *42*(18), 7374-7382.

Duverger, C., Lambotte, S., Bernard, P., Lyon-Caen, H., Deschamps, A., & Nercessian, A. (2018). Dynamics of microseismicity and its relationship with the active structures in the western Corinth Rift (Greece). *Geophysical Journal International*, *215*(1), 196-221.

Dyer, B., R. Baria, et S. Michelet. 2004. « Soultz GPK3 stimulation and GPK3-GPK2 circulation May to July 2003 - Seismic monitoring report ». Report n° EEIG 05/2004. Semore Seismic for Socomine.

Edwards, B., & Douglas, J. (2014). Magnitude scaling of induced earthquakes. *Geothermics*, *52*, 132-139.

Fischer, T., & Hainzl, S. (2017). Effective stress drop of earthquake clusters. *Bulletin of the Seismological Society of America*, *107*(5), 2247-2257.

Fischer, T., & Hainzl, S. (2021). The growth of earthquake clusters. *Frontiers in Earth Science*, *9*, 79.

Gao, H., Schmidt, D. A., & Weldon, R. J. (2012). Scaling relationships of source parameters for slow slip events. *Bulletin of the Seismological Society of America*, *102*(1), 352-360.

Gerard, A., Baumgärtner, J., Baria, R., & Jung, R. (1997). An attempt towards a conceptual model derived from 1993−1996 hydraulic operations at Soultz. In Proceedings of NEDO International Symposium, Sendai, Japan (Vol. 2, pp. 329–341).

Glowacka, E., González, J. J., Nava, F. A., Farfan, F., & Diaz de Cossio, G., Monitoring surface deformations in the Mexicali valley, BC, Mexico Proceedings of tenth international symposium on deformation measurements (Vol. 175183) (2001)

Goebel, T. H., & Brodsky, E. E. (2018). The spatial footprint of injection wells in a global compilation of induced earthquake sequences. *Science*, *361*(6405), 899-904.

Goertz-Allmann, B. P., Goertz, A., and Wiemer, S. (2011), Stress drop variations of induced earthquakes at the Basel geothermal site, *Geophys. Res. Lett.*, 38, L09308,

Gualandi, A., Nichele, C., Serpelloni, E., Chiaraluce, L., Anderlini, L., Latorre, D., ... & Avouac, J. P. (2017). Aseismic deformation associated with an earthquake swarm in the northern Apennines (Italy). *Geophysical Research Letters*, *44*(15), 7706-7714.

Guglielmi, Y., Cappa, F., Avouac, J. P., Henry, P., & Elsworth, D. (2015). Seismicity triggered by fluid injection–induced aseismic slip. *Science*, *348*(6240), 1224-1226.

Hainzl, S., & Fischer, T. (2002). Indications for a successively triggered rupture growth underlying the 2000 earthquake swarm in Vogtland/NW Bohemia. *Journal of Geophysical Research: Solid Earth*, *107*(B12), ESE-5.

Hawthorne, J. C., & Rubin, A. M. (2013). Laterally propagating slow slip events in a rate and state friction model with a velocity-weakening to velocity-strengthening transition. *Journal of Geophysical Research: Solid Earth*, *118*(7), 3785-3808.

Hawthorne, J. C., Ampuero, J. P., & Simons, M. (2017). A method for calibration of the local magnitude scale based on relative spectral amplitudes, and application to the San Juan Bautista, California, area. *Bulletin of the Seismological Society of America*, *107*(1), 85-96.

Herrmann, M., Kraft, T., Tormann, T., Scarabello, L., & Wiemer, S. (2019). A consistent high-resolution catalog of induced seismicity in Basel based on matched filter detection and tailored post-processing. *Journal of Geophysical Research: Solid Earth*, *124*(8), 8449-8477.

Hincks, T., Aspinall, W., Cooke, R., & Gernon, T. (2018). Oklahoma's induced seismicity strongly linked to wastewater injection depth. *Science*, *359*(6381), 1251-1255.

Hong, T. K., Park, S., Lee, J., Chung, D., & Kim, W. (2020). One-off deep crustal earthquake swarm in a stable intracontinental region of the southwestern Korean Peninsula. *Physics of the Earth and Planetary Interiors*, *308*, 106582.

Houston, H., Delbridge, B. G., Wech, A. G., & Creager, K. C. (2011). Rapid tremor reversals in Cascadia generated by a weakened plate interface. *Nature Geoscience*, *4*(6), 404-409.

Ide, S., Beroza, G. C., Shelly, D. R., & Uchide, T. (2007). A scaling law for slow earthquakes. *Nature*, *447*(7140), 76-79.

Ito, Y., Obara, K., Shiomi, K., Sekine, S., & Hirose, H. (2007). Slow earthquakes coincident with episodic tremors and slow slip events. *Science*, *315*(5811), 503-506.

Jenatton, L., Guiguet, R., Thouvenot, F., & Daix, N. (2007). The 16,000-event 2003–2004 earthquake swarm in Ubaye (French Alps). *Journal of Geophysical Research: Solid Earth*, *112*(B11).

Kim, W. Y. (2013). Induced seismicity associated with fluid injection into a deep well in Youngstown, Ohio. *Journal of Geophysical Research: Solid Earth*, *118*(7), 3506-3518.

Kwiatek, G., Saarno, T., Ader, T., Bluemle, F., Bohnhoff, M., Chendorain, M., ... & Wollin, C. (2019). Controlling fluid-induced seismicity during a 6.1-km-deep geothermal stimulation in Finland. *Science advances*, *5*(5), eaav7224.

Lambert, V., Lapusta, N., & Faulkner, D. (2021). Scale dependence of earthquake rupture prestress in models with enhanced weakening: implications for event statistics and inferences of fault stress. *Earth and Space Science Open Archive*, 55.

Larochelle, S., Lapusta, N., Ampuero, J. P., & Cappa, F. (2021). Constraining Fault Friction and Stability With Fluid-Injection Field Experiments. *Geophysical Research Letters*, e2020GL091188.

Lengliné, O., Lamourette, L., Vivin, L., Cuenot, N., & Schmittbuhl, J. (2014). Fluid-induced earthquakes with variable stress drop. *Journal of Geophysical Research: Solid Earth*, *119*(12), 8900-8913.

Lengliné, O., Boubacar, M., & Schmittbuhl, J. (2017). Seismicity related to the hydraulic stimulation of GRT1, Rittershoffen, France. *Geophysical Journal International*, *208*(3), 1704-1715

Lohman, R. B., & McGuire, J. J. (2007). Earthquake swarms driven by aseismic creep in the Salton Trough, California. *Journal of Geophysical Research: Solid Earth*, *112*(B4).

Madariaga, R. Dynamics of an expanding circular fault. *Bulletin of the Seismological Society of America*, *66*(3), 639-666.(1976)

Matsuzawa, T., Uchida, N., Igarashi, T., Okada, T., & Hasegawa, A. (2004). Repeating earthquakes and quasi-static slip on the plate boundary east off northern Honshu, Japan. *Earth, planets and space*, *56*(8), 803-811.

McGarr, A., & Barbour, A. J. (2018). Injection-induced moment release can also be aseismic. *Geophysical Research Letters*, *45*(11), 5344-5351.

Passarelli, L., Rivalta, E., Jónsson, S., Hensch, M., Metzger, S., Jakobsdóttir, S. S., ... & Dahm, T. (2018). Scaling and spatial complementarity of tectonic earthquake swarms. *Earth and Planetary Science Letters*, *482*, 62-70.

Passelègue, F. X., Almakari, M., Dublanchet, P., Barras, F., Fortin, J., & Violay, M. (2020). Initial effective stress controls the nature of earthquakes. *Nature communications*, *11*(1), 1-8.

Peng, Z., & Gomberg, J. (2010). An integrated perspective of the continuum between earthquakes and slow-slip phenomena. *Nature geoscience*, *3*(9), 599-607.

Roland, E., & McGuire, J. J. (2009). Earthquake swarms on transform faults. *Geophysical Journal International*, *178*(3), 1677-1690.

Ross, Z. E., Cochran, E. S., Trugman, D. T., & Smith, J. D. 3D fault architecture controls the dynamism of earthquake swarms. *Science*, *368*(6497), 1357-1361. (2020)

Rubin, A. M. (2008). Episodic slow slip events and rate-and-state friction. *Journal of Geophysical Research: Solid Earth*, *113*(B11).

Schmidt, D. A., & Gao, H. (2010). Source parameters and time-dependent slip distributions of slow slip events on the Cascadia subduction zone from 1998 to 2008. *Journal of Geophysical Research: Solid Earth*, *115*(B4).

Seeber, L., Armbruster, J. G., & Kim, W. Y. (2004). A fluid-injection-triggered earthquake sequence in Ashtabula, Ohio: Implications for seismogenesis in stable continental regions. *Bulletin of the Seismological Society of America*, *94*(1), 76-87.

Shapiro, S. A., Huenges, E., & Borm, G. (1997). Estimating the crust permeability from fluid-injection-induced seismic emission at the KTB site. *Geophysical Journal International*, *131*(2), F15-F18.

Uchida, N. (2019). Detection of repeating earthquakes and their application in characterizing slow fault slip. *Progress in Earth and Planetary Science*, *6*(1), 1-21.

Wei, et al., The 2012 Brawley swarm triggered by injection-induced aseismic slip Earth and Planetary Science Letters 422, 115 (2015).

Wynants-Morel, N., Cappa, F., De Barros, L., & Ampuero, J. P. (2020). Stress perturbation from aseismic slip drives the seismic front during fluid injection in a permeable fault. *Journal of Geophysical Research: Solid Earth*, *125*(7), e2019JB019179.

Yeck, W. L., Block, L. V., Wood, C. K., & King, V. M. (2015). Maximum magnitude estimations of induced earthquakes at Paradox Valley, Colorado, from cumulative injection volume and geometry of seismicity clusters. *Geophysical Journal International*, *200*(1), 322-336.